Licochalcone-A Induces Intrinsic and Extrinsic Apoptosis via ERK1/2 and p38 Phosphorylation-mediated TRAIL Expression in Head and Neck Squamous Carcinoma FaDu Cells

Mi-Ra Park[a,f,1], **Su-Gwan Kim**[a,b,1], **In-A Cho**[a,b], **Dahye Oh**[a,b], **Kyeong-Rok Kang**[a,b], **Sook-Young Lee**[a,b], **Sung-Min Moon**[a], **Seung Sik Cho**[c], **Goo Yoon**[c], **Chun Sung Kim**[a], **Ji-Su Oh**[a,b], **Jae-Seek You**[a], **Do Kyung Kim**[a,b], **Yo-Seob Seo**[a], **Hee-Jeong Im**[d], and **Jae-Sung Kim**[e,*]

[a]Oral Biology Research Institute, Chosun University, Gwangju, 501-759, Republic of Korea

[b]Regional Innovation Center for Dental Science and Engineering, Chosun University, Gwangju, 501-759, Republic of Korea

[c]Department of Pharmacy, College of Pharmacy, Mokpo National University, Muan, Jeonnam, 353-729, Republic of Korea

[d]Department of Biochemistry, Rush University Medical Center, Chicago, IL60612, USA

[e]The Division of Natural Medical Sciences, College of Health Science, Chosun University, Gwangju, 501-759, Republic of Korea

[f]Department of Biomedical Science, CHA University, Seongnam, Gyeongghi-do, 487-101, Republic of Korea

Abstract

We investigated Licochalcone-A (Lico-A)-induced apoptosis and the pathway underlying its activity in a pharyngeal squamous carcinoma FaDu cell line. Lico-A purified from root of *Glycyrrhiza inflata* had cytotoxic effects, significantly increasing cell death in FaDu cells. Using a cell viability assay, we determined that the IC_{50} value of Lico-A in FaDu cells was approximately 100 μM. Chromatin condensation was observed in FaDu cells treated with Lico-A for 24 h. Consistent with this finding, the number of apoptotic cells increased in a time-dependent manner when FaDu cells were treated with Lico-A. TRAIL was significantly up-regulated in Lico-A-treated FaDu cells in a dose-dependent manner. Apoptotic factors such as caspases and PARP polymerase were subsequently activated in a caspase-dependent manner. In addition, levels of pro-apoptotic factors increased significantly in response to Lico-A treatment, while levels of anti-apoptotic factors decreased. Lico-A-induced TRAIL expression was mediated in part by a MAPK signaling pathway involving ERK1/2 and p38. Lastly, in an *in vivo* xenograft mouse model, Lico-A treatment effectively suppressed the growth of FaDu cell xenografts by activating caspase-3, without affecting the body weight of mice. Taken together, these data suggest that Lico-A has

*Correspondence to: Jae-Sung Kim, Ph.D., Assistant Professor, The Division of Natural Medical Sciences, College of Health Science, Chosun University, 375 Seosuk-dong, Dong-gu, Gwangju 501-759, Republic of Korea., Tel.: +82-62-230-6870; Fax: +82-62-230-6870; js_kim@chosun.ac.kr.
[1]MR Park and SG Kim contributed equally to this work

Conflict of Interest

The authors declare that there are no conflicts of interest.

potential chemopreventive effects and should therefore be developed as a chemotherapeutic agent for pharyngeal squamous carcinoma.

Keywords

Pharyngeal squamous carcinoma; Licochalcone-A; FaDu cells; Apoptosis; Chemoprevention

1. Introduction

Head and neck squamous cell carcinoma (HNSCC), which originates from the mucosal epithelium of the head and neck, is one of the most common cancers. HNSCC is associated with a high mortality rate and approximately 640,000 cases are reported annually worldwide (Jemal et al., 2011; Lacko et al., 2014). The major etiological factors of HNSCC include tobacco (Rothman, 1978) and alcohol consumption (Maier et al., 1992), betel nut chewing (Lin et al., 2005), and human papillomavirus infection (Tao and Chan, 2007; Vidal and Gillison, 2008). Although clinical interventions such as surgery, radiotherapy, chemotherapy, and chemo-radiotherapy have advanced recently, the 5-year survival rate of HNSCC patients remains poor and morbidity is high. Survival and morbidity rates have not improved significantly in the last 30 years (Vigneswaran et al., 2011). Thus, clinical management strategies for HNSCC are urgently needed, requiring the development of chemotherapeutic agents with greater efficacy and fewer side effects.

Current strategies for developing chemotherapeutic agents rely on inducing apoptosis in cancer cells (Fesik, 2005). Apoptosis, programmed cell death, is characterized by cell shrinkage (McCarthy and Cotter, 1997), chromatin condensation (Dobrucki and Darzynkiewicz, 2001), cellular protein and DNA degradation (van Loo et al., 2001), and apoptotic body formation, which are triggered by various anti-tumorigenic cellular mechanisms (Lin et al., 2012). Cell suicide processes are precisely regulated by extrinsic and intrinsic apoptotic pathways that are death receptor-dependent and mitochondria-dependent, respectively (Hensley et al., 2013). The death receptor-dependent extrinsic apoptosis pathway is usually triggered by the interaction between death receptors on the cell surface and its specific ligands such as the Fas ligand (FasL or CD95L) (Weissmann, 1994) and Tumor Necrosis Factor (TNF)-related apoptosis-inducing ligand (TRAIL) (Li et al., 2006). Fas-associated protein with death domain (FADD), a Fas receptor adaptor molecule, subsequently induces the cleavage of extrinsic apoptotic factors such as caspase-8, caspase-3, and poly (ADP ribose) polymerase (PARP) (Ikner and Ashkenazi, 2011), eventually inducing apoptotic changes and cell death. The mitochondrial-dependent intrinsic apoptotic pathway is triggered by caspase-8, which is activated by the extrinsic apoptotic pathway or the loss of mitochondrial transmembrane potential. Activated caspase-8 leads to the loss of mitochondrial transmembrane potential by cleaving the cytosolic BH3-interacting domain death agonist (BID) to truncated BID (tBID), a pro-apoptotic regulator that promotes the insertion of Bax into the outer mitochondrial membrane (Li et al., 1998). Anti-apoptotic factors such as B-cell lymphoma 2 (Bcl-2) and B-cell lymphoma extra-large (Bcl-xL) are downregulated or pro-apoptotic factors such as Bcl-2-associated X protein (Bax) and Bcl-2-associated death promoter (BAD) are significantly up-regulated during activation of

the mitochondria-dependent intrinsic apoptotic pathway (Fischer et al., 2003; Zhu et al., 2005). Procaspase-9 and -3 as well as PARP are then cleaved to induce cell death. Therefore, apoptosis has emerged as a critical target for anticancer clinical chemotherapeutic agents such as those developed from medicinal plants.

Recently, several natural compounds with anticancer activity have been approved as clinical chemotherapeutic agents by the United States Food and Drug Administration (Kinghorn et al., 2011). Biologically active compounds isolated from medicinal plants have received considerable interest as potential clinical chemotherapeutic drugs because of their effective anticancer effects and potentially fewer side effects; therefore, natural compounds are considered a promising strategy for cancer treatment and prevention.

Licorice, the root of *Glycyrrhiza* species, is a plant used in folk and oriental medicines for stomach ulcers, bronchitis, and sore throats (Wittschier et al., 2009). The main active ingredient in licorice is Licochalcone-A (Lico-A; (E)-3-[4-hydroxy-2-methoxy-5-(2-methylbut-3-en-2-yl)phenyl]-10-(4-hydroxyphenyl)prop-2-en-1-one), a natural phenolic chalconoid (Cho et al., 2014). According to recent studies, Lico-A has antioxidant (Fu et al., 2013), antiviral (Adianti et al., 2014), anti-inflammatory (Chu et al., 2012; Fu et al., 2013), antimicrobial (Messier and Grenier, 2011), antimalarial (Mishra et al., 2009), antiangiogenic (Kim et al., 2010), and osteogenic activities (Kim et al., 2012). Furthermore, Lico-A reportedly has anticancer activity in various cancers types such as oral (Kim et al., 2014), bladder (Yuan et al., 2013), ovarian (Lee et al., 2012), gastric (Xiao et al., 2011), colon (Lee et al., 2008), and prostate (Fu et al., 2004; Yo et al., 2009) cancer as well as in hepatocellular carcinoma (Choi et al., 2014). Although the antitumor effects and cellular mechanism of Lico-A activity have been investigated in various cancers, little is known regarding its effect on HNSCC.

Therefore, in this study, we aimed to determine whether Lico-A could function as a chemotherapeutic agent for HNSCC. Furthermore, we evaluated the potential apoptotic effect of Lico-A on HNSCC and elucidated the apoptotic signaling pathway induced by Lico-A.

2. Materials and methods

2.1. Cell culture

Normal human oral keratinocytes (hNOKs) were purchased from ScienCell Research Laboratories (Carlsbad, CA, USA). The hNOKs were maintained in Dulbecco's modified Eagle's medium (Life Technologies, Grand Island, NY, USA) containing 10% fetal bovine serum (FBS) (Life Technologies, Grand Island, NY, USA). FaDu cells, a human pharyngeal squamous carcinoma cell line, were obtained from the American Type Culture Collection and cultured according to the instructions provided. FaDu cells were maintained in minimum essential medium (Life Technologies, Grand Island, NY, USA) containing 10% FBS. Cells were grown in a humidified incubator at 37°C in 5% CO_2.

2.2. Cell viability assay

The cells were seeded at a density of 1×10^5 cells/mL in 96-well plates and allowed to attach to the well overnight. After incubation, cultured cells were treated with 0, 25, 50, 100, and 125 μM Lico-A for 24 h at 37°C to determine its dose-dependent effects. After incubation under the defined conditions, cells were incubated for another 4 h in 20 μL of 5 mg/mL 3-(4,5-dimethylthiazol-2-yl)-2,5-diphenyltetrazolium bromide (MTT) (Life Technologies, Grand Island, NY, USA). The supernatant was subsequently removed, and MTT crystals were dissolved in 200 μL/well dimethyl sulfoxide. Thereafter, optical density was measured at 570 nm using a spectrometer. Experiments were performed at least three times.

2.3. Cell survival assay

Cell survival was measured as previously described (Kim et al., 2012a), using calcein green AM and ethidium homodimer-1 (Life Technologies, Grand Island, NY, USA) to stain live and dead cells, respectively. To evaluate cell survival, FaDu cells and hNOKs were plated on chamber slides, stimulated with Lico-A for 24 h, and then stained with calcein green AM and ethidium homodimer-1 as according to the manufacturer's protocol. Cells were then examined and imaged using a fluorescence microscopy (Eclipse TE200; Nikon Instruments, Melville, NY).

2.4. Quantification of apoptosis

Detection of apoptotic cells was accomplished by fluorescently staining DNA to examine chromosomal condensation. 1×10^5 cells/mL plated in chamber were treated with 0, 100, and 125 μM Lico-A and incubated for 24 h. Cells were stained with 4′-6-diamidino-2-phenylindole (DAPI) (Sigma-Aldrich, St. Louis, MO, USA) and then examined and photographed using fluorescence microscopy (Eclipse TE200; Nikon Instruments, Melville, NY).

2.5. Flow cytometric analysis

Flow cytometric analysis was performed on cells co-stained with annexin V-FITC and propidium iodide (PI) (Cell signaling Technology, Danvers, MA, USA) to detect apoptosis. After 5×10^5 cells/mL of FaDu cells were plated into a 6-well plate. After 24 h, the cells were treated with Lico-A for 12 and 24 h. Both floating and attached cells were then collected, washed twice with ice-cold phosphate-buffered saline, and resuspended in 500 μL of 1× binding buffer (BD Biosciences, San Diego, CA, USA). Annexin V-FITC and PI were added to the cells for 15 min at 37°C in the dark. The population of Annexin-V-positive cells and the cell cycle phase were analyzed using a BD Cell Quest® version 3.3 instrument (Becton Dickinson, San José, CA, USA) and WinMDI version 2.9 software (The Scripps Research Institute, San Diego, CA, USA).

2.6. Western blot analysis

Cells (5×10^6 cells per well) were plated on culture dishes. After treatment of Lico-A for 24 h, cells were then harvested, lysed using cell lysis buffer (Cell signaling Technology, Danvers, MA, USA) containing protease and phosphatase inhibitor cocktails, and incubated

for 1 h at 4°C. Lysates were centrifuged at $14,000 \times g$ for 10 min at 4°C. The supernatant was used as the cytosolic fraction. Total protein concentrations of the cell lysates were determined by bicinchoninic acid protein assays (Thermo Scientific, Rockford, IL, USA). In addition, conditioned media collected to detect the TRAIL secreted from FaDu cells treated with Lico-A. Into equal amounts of protein and conditioned media, 5× loading buffer was added and the mixture was boiled at 90°C for 10 min. Both proteins and conditioned media were separated using sodium dodecyl sulfate polyacrylamide gel electrophoresis (SDS-PAGE) and transferred into nitrocellulose membranes. After blocking for 2 h with 5% bovine serum albumin in Tris-buffered saline containing Tween-20 at room temperature, membranes were incubated with primary antibody at 4°C overnight and then incubated with horseradish peroxidase-conjugated secondary antibody. The following antibodies were used: antibodies against TRAIL, cleaved caspases (3, 7, 8, and 9), Bid, Bcl-2, Bcl-xL, p53, Bax, Bad, Apaf-1, PARP, β-actin, phospho-ERK, total ERK, phospho-p38, total p-38, phospho-JNK, and total JNK were purchased from Cell Signaling Technology (Danvers, MA, USA). The immunoreactive bands were visualized using the ECL System (Amersham Biosciences, Piscataway, NJ) and were exposed on radiographic film.

2.7. Caspase-3/-7 activity assay

The activity of the apoptosis executioner caspase-3/-7 was determined using the cell-permeable fluorogenic substrate PhiPhiLux-G1D2 (OncoImmunin Inc.; Gaithersburg, MD, USA) according to the manufacturer's instructions and was and photographed using fluorescence microscopy (Eclipse TE200; Nikon Instruments, Melville, NY).

2.8. Caspase dependent cell survival assay

The cells were plated at a density of 1×10^5 cells/mL in 96-well plates and allowed to attach to the well overnight. After incubation, cultured cells were treated with 100 µM Lico-A in presence or absence of 20 µM of caspase-3 inhibitor (Z-VAD-FMK), 20 µM of caspase-8 inhibitor (Z-IETD-FMK) or 20 µM of caspase-9 inhibitor (Z-LEHD-FMK) were incubated for 24 h at 37°C. After incubation under the defined conditions, cell cytotoxicity was measured by MTT assay.

2.9. Xenograft mouse model

All animal studies were performed the protocol (CDMDIRB-1216-A94) approved by the Institutional Animal Care and Use Committee (IACUC) of Chosun University. Five-week-old male nude mice, each weighing approximately 20 g, were divided into a xenografted positive control group ($n = 5$) and xenografted experimental group ($n = 5$) in which the anticarcinogenic effect of Lico-A was tested. According to the previously reported method to generate the xenograft animal model with FaDu squamous cell carcinoma (Brake et al., 2008), cells at a concentration of 1×10^7 cells/100 µL were injected subcutaneously into the right and left flanks of each of the control and experimental mice, respectively. After tumor formation (approximately 1,000 mm³) was detected under the skin of mice that had received FaDu cell xenographs, 10 mg/kg of Lico-A dissolved in 5% ethanol and 5% ethanol without Lico-A was injected intraperitoneally into experimental and controls groups, respectively, three times per week for 8 consecutive weeks. Tumor sizes were measured weekly using a

vernier caliper for 8 weeks following FaDu cell xenografting. Body weights were also recorded weekly. At the end of the study, all of the xenografted animals were perfused with saline and were fixed in 4% paraformaldehyde. Finally, tumor masses were dissected surgically and embedded in paraffin for immunohistological analysis.

2.9. Histology and Immunohistochemistry

The experimental animals were euthanized using an overdose of inhaled anesthesia according to the protocol approved by IACUC at School of Dentistry, Chosun University. Briefly, tumor masses were excised, post-fixed in 4% paraformaldehyde for 7 day, dehydrated in a series of ethanol solutions (50, 70, 95, and 100%; 15 min per step), and then submerged in xylene twice for 10 min. Paraffin-embedded tissue blocks were prepared and cut using a microtome. The 5-μm-thick sections were placed on glass slides. The sections were deparaffinized using two changes of xylene for 10 min, rehydrated with two washes each of 100% and 95% ethanol for 1 min, and then rinsed with tap water for 10 min. The sections were incubated at 4°C with cleaved capase-3 antibody overnight and incubated for 1 h at room temperature with peroxidase-conjugated goat anti-mouse antibody. Sections were subsequently counterstained using hematoxylin and eosin, transferred to mounting reagent, and examined by microscopy.

2.10. Statistical analysis

The experimental data are presented as the mean ± standard deviation from at least three independent experiments and were compared using analysis of variance, followed by Student's t-tests. A p value of less than 0.05 was considered statistically significant.

3. Results

3.1. Lico-A has cytotoxic effects on FaDu cancer cells, but does not affect hNOK viability

To assess the cytotoxic effects of Lico-A on FaDu cells and hNOKs, cells were treated with various concentrations of Lico-A for 24 h. After incubation, cell viability was assessed using an MTT assay. As shown in Fig. 1A (left panel), cytotoxicity was not observed in hNOKs treated with Lico-A (25–125 μM). In contrast, the survival rate of FaDu cells decreased significantly in response to Lico-A in a dose-dependent manner (Fig. 1A, right panel). The IC_{50} value of Lico-A in FaDu cells was calculated as ~100 μM. To confirm the cytotoxicity of Lico-A in FaDu cells, we performed a cell survival assay to visualize both live and dead cells stained with calcein green AM and ethidium homodimer-1, respectively. In addition, primary hNOKs treated with 100 μM Lico-A for 24 h were stained green by membrane permeable calcein AM, which is cleaved by cytosolic esterases in living cells. In contrast, a significant number of dead cells stained red by ethidium homodimer-1 were observed in FaDu cells treated with 100 μM Lico-A. These data demonstrated that Lico-A had cytotoxic effects specifically in FaDu cancer cells (Supplementary Fig. 1).

3.2. Lico-A induces apoptotic cell death in FaDu cancer cells

To elucidate the cellular mechanism by which Lico-A induced FaDu cell death, we performed DAPI staining to detect chromatin condensation, an indicator of apoptotic cell death. Chromatin condensation was induced in FaDu cells treated with Lico-A in a dose-

dependent manner (Supplementary Fig. 2). To determine whether Lico-A-induced cell death was mediated by apoptosis or necrosis, flow cytometric analysis was performed to detect apoptotic cell death by using annexin V/PI co-staining, which specifically labels apoptotic cells. As shown in Fig. 1B, the apoptotic population increased gradually to approximately 32.12% and 35.65% in FaDu cells stimulated with 100 μM Lico-A for 12 and 24 h, respectively. Therefore, these data suggest that Lico-A induces FaDu cell death through an apoptotic mechanism.

3.3. Lico-A induced cell death is caspase-dependent through both extrinsic and intrinsic apoptotic pathways

To determine the apoptotic pathway induced by Lico-A, immunoblotting was performed to identify the activation and/or expression of several pro-apoptotic and anti-apoptotic factors. FaDu cells were treated with 50 and 100 μM Lico-A for 24 h. As shown in Fig. 2A, expression of the apoptosis-inducing ligand TRAIL (28 kDa) was up-regulated significantly as dose-dependent manner in both FaDu cells treated with Lico-A and its conditioned media. Up-regulated TRAIL activated caspase-8 (43 kDa, 41 kDa, and 18 kDa), an apoptotic factor associated with death receptor-dependent extrinsic apoptotic signaling (Fig. 2B). Activated caspase-8 induced apoptosis in FaDu cells through activating caspase-7.

Activated caspase-8 also triggered the mitochondria-dependent intrinsic apoptotic signaling pathway in FaDu cells stimulated with Lico-A by cleaving BID (22 kDa) to tBID (15 kDa) (Fig. 2C). In addition, the anti-apoptotic factors Bcl-2 (26 kDa) and Bcl-xL (26 kDa) were down-regulated in FaDu cells in response to Lico-A treatment, whereas the known tumor suppressor p53 was up-regulated significantly. In contrast, pro-apoptotic factors including Bax (21 kDa), Bad (24 and 46 kDa), and apoptotic protease activating factor 1 (Apaf-1, 130 kDa) were up-regulated in response to Lico-A treatment. Up-regulated Apaf-1 subsequently induced the cleavage of caspase-9 (37 kDa), which in turn induced sequential cleavage of caspase-3 (17 and 19 kDa) and PARP (89 kDa). Moreover, activated caspase-8 and caspase-9 both activated caspase-3 (17 and 19 kDa) and PARP (89 kDa), and then induced apoptosis (Fig. 2D). Taken together, these data suggest that Lico-A-induced FaDu cancer cell death is mediated by both death receptor-dependent extrinsic and mitochondria-dependent intrinsic apoptotic pathways.

The activation of caspases is a key feature of apoptotic signaling pathways. Therefore, to confirm that Lico-A-induced apoptosis is mediated by caspase activation, we performed a caspase-3/-7 activation assay in FaDu cells treated with Lico-A by using PhiPhiLux, a fluorogenic caspase substrate. As shown in Fig. 3A, caspase-3/-7 activation was higher in FaDu cells treated with 50 μM and 100 μM Lico-A than in non-treated control cells. Lico-A-induced caspase-3 activation in FaDu cells was reduced significantly by the presence of 20 μM of the pan-caspase inhibitor Z-VAD-FMK (Fig. 3B). In order to confirm the contribution of extrinsic and intrinsic signaling pathway in Lico-A-induced cell death is a caspase-dependent apoptosis, we measured the cell viability of FaDu cells treated with 100 μM Lico-A in presence or absence of 20 μM Z-VAD-FMK (pan-caspase inhibitor), 20 μM Z-IETD-FMK (caspase-8 inhibitor for the inhibition of death receptor dependent extrinsic apoptosis signaling pathway) or 20 μM Z-LEHD-FMK (caspase-9 inhibitor for the inhibition

of mitochondria dependent intrinsic apoptosis signaling pathway). As shown in Fig. 3C, pan-caspase inhibitor Z-VAD-FMK effectively rescued up to $83\pm14.6\%$ compared with Lico-A-induced cell cytotoxicity ($48\pm6.4\%$). Furthermore, in the presence of Z-IETD-FMK or Z-LEHD-FMK, Lico-A-induced cell cytotoxicity in FaDu cell was counteracted by $\sim72\pm6.4\%$ and $\sim65\pm6.25\%$, respectively. Therefore, these are suggesting that Lico-A-induced FaDu cell apoptosis is dependent on caspases activated by both extrinsic and intrinsic apoptotic pathways.

3.4. Lico-A-induced TRAIL expression in FaDu cancer cells is induced by ERK and p38 MAPK signaling pathways

To determine the cellular signaling pathway of Lico-A induced TRAIL expression in FaDu cancer cells, we examined the activation of mitogen-activated protein kinase (MAPK) signaling pathways that have previously been linked to Lico-A-mediated TRAIL expression in the KB human oral cancer cell line (Kim et al., 2014). As shown in Fig. 4A, 100 μM Lico-A led to ERK1/2 (42 kDa and 44 kDa, respectively) and p38 (38 kDa) activation within 5 min of treatment, as indicated by the phosphorylation of these protein. Activation was sustained for approximately 30 min after treatment. In contrast, Lico-A did not affect JNK phosphorylation (54 kDa and 46 kDa) in FaDu cells. To determine which pathway underlies Lico-A-induced TRAIL expression, FaDu cells were co-treated with 100 μM Lico-A and either 25 μM PD98059 (ERK1/2 MAPK pathway inhibitor) or 5 μM SB203580 (p38 MAPK pathway inhibitor). As shown in Fig. 4B, Lico-A-induced TRAIL (28 kDa) expression was suppressed in the presence of either ERK1/2 or p38 pathway-specific inhibitors. Pro-apoptotic factors such as caspase-8 (43 kDa, 41 kDa and 18 kDa), caspase-9 (37 kDa), caspase-3 (19 kDa and 17 kDa) and PARP (89 kDa) that act downstream of TRAIL were inactivated in the presence of either inhibitor. Moreover, the Lico-A-induced reductions in cell viability were rescued in by ERK1/2 and p38 inhibitor treatments (Fig. 4C). Thus, these data suggest that Lico-A-induced TRAIL expression is meditated by the activation of ERK1/2 and p38 MAPK signaling pathways in FaDu cancer cells.

3.5. Lico-A suppresses tumor formation in a FaDu cancer cell xenograft animal model

To assess the effects of Lico-A on FaDu tumor growth, FaDu cells were xenografted into experimental animals (mice) and the resulting tumor sizes and body weights were measured weekly for up to 8 weeks. As shown in Fig. 5A, tumor volumes were significantly lower in mice that received 10 mg/kg Lico-A treatment compared to those in the control group. No obvious loss of body weight was observed (Fig. 5B), indicating that Lico-A was well tolerated. Moreover, immunohistochemical analysis of the tumors showed that caspase-3 expression was markedly higher in Lico-A-treated tumors than in control tumors (Fig. 5C).

4. DISSCUSION

HNSCC is known to be one of the most fatal cancers worldwide and shows a high frequency of recurrence (Huang et al., 2013). Although curative clinical management strategies for HNSCC exist, including surgical interventions, radiotherapy, and chemotherapy, the 5-year survival rate of HNSCC patients is approximately only 50–60% (Osthus et al., 2013). Moreover, survivors experience temporal or permanent side effects including

osteoradionecrosis as well as discomfort in chewing, swallowing, and speaking (Chang et al., 2012). Although combinational chemotherapies are currently considered the primary clinical treatments for various cancer types, this approach is limited because of clinical side effects such as high toxicity and drug tolerance (Hadden, 1997). Therefore, the development of chemotherapeutic agent with fewer side effects is urgently needed for cancer patients. In an attempt to develop chemotherapeutic agents with fewer side effects, the anticancer activities and cellular mechanisms of natural compounds isolated from medicinal plants used in orthodox traditional medicine are currently being investigated for various cancer types (Hsan et al., 2010). Therefore, we investigated whether Lico-A isolated from *Glycyrrhiza* species medicinal plants induced apoptosis in FaDu cells and elucidated the cellular mechanism underlying its activity in the present study.

Candidate chemotherapeutic compounds must not only have low cytotoxicity in normal cells, but also must induce highly specific cancer cell death. According to this prerequisite for use as a chemotherapeutic agent, the cytotoxicity of Lico-A was tested in primary hNOK by performing MTT and cell survival assays. Cell cytotoxicity assessed by MTT assay was not observed in the primary hNOK cultures treated with 25–125 μM Lico-A for 24 h. Moreover, Park et al., reported recently that Lico-A slightly stimulated the growth of normal IEC-6 intestinal epithelial cells and CCD118SK fibroblast without cell toxicity (Park et al., 2014). Furthermore, Tsai et al., showed that Lico-A did not affect the cell viability in normal hepatic cells (Tsai et al., 2014). Therefore, these are consistently suggesting that Lico-A may have either potential biological safety or purportedly minimized cytotoxicity in normal cells.

However, the viability of FaDu cells gradually decreased by Lico-A in a dose-dependent manner. Treatment with 100 and 125 μM Lico-A decreased FaDu cell viability by 50% and 80%, respectively, compared to the non-treated control. Although Zheng et al., reported that the IC_{50} value of Lico-A was estimated at approximately 300 μM in the human oral cancer SCC-25 cells (Zeng et al., 2014), the IC_{50} value of Lico-A in FaDu cells was estimated at approximately 100 μM, a higher IC_{50} value than the 50 μM IC_{50} reported for KB human oral cancer cells (Kim et al., 2014). However, IC_{50} values of Lico-A was estimated at various dose ranges in other cancer cells. For example, Xiao et al., reported that IC_{50} values of Lico-A were estimated approximately 40 μM gastric cancer cell lines such as MKN-28, AGS, and MKN-45 (Xiao et al., 2011). Furthermore, IC_{50} values of Lico-A were estimated approximately 60 μM in human bladder cancer T24 cells (Yuan et al., 2013), approximately 10 μM in human hepatocellular liver carcinoma cell HepG2 and approximately 20 μM in both human hepatoma cell lime Hep3B and SNU-878 (Choi et al., 2014). Therefore, these are showing that IC_{50} value of Lico-A might be dependent on the cell specificity.

Recently, Kim et al. (2014) reported that Lico-A increased KB human oral cancer cell viability gradually, but did not affect the hNOK viability (Kim et al., 2014). To confirm that Lico-A had cancer cell-specific cytotoxic effects, we performed a cell survival assay. In the hNOK cells treated with 100 μM Lico-A for 24 h, nearly all of the cells were stained green by the membrane-permeable calcein green AM, which is cleaved by esterases in live cells to yield cytoplasmic green fluorescence. In contrast, 100 μM Lico-A decreased the overall number of FaDu cells and increased the number of cells stained red by the membrane-impermeable cell death marker ethidium homodimer-1. Taken together, these data suggest

that Lico-A exhibits cancer cell-specific cytotoxicity and has potential less side effects as a potential chemotherapeutic agent.

Next, to clarify the mechanism by which Lico-A induced FaDu cell death, we performed DAPI staining to examine alterations in chromatin condensation. The number of FaDu cells with condensed chromatin gradually increased in response to Lico-A in a dose-dependent manner. Chromatin condensation is a hallmark of apoptotic cell death (Tounekti et al., 1995). Therefore, these results suggested that Lico-A induced the apoptosis of FaDu cells. To verify whether Lico-A induced apoptosis in FaDu cells, flow cytometric analysis was performed on cells co-stained with PI and annexin V. An indicator of apoptotic cell death is the exposure of membrane phospholipids to the external cellular environment. Annexin V is a calcium-dependent phospholipid binding protein that has high affinity for phosphatidylserine, which is translocated from the inner to the outer cellular membrane during in apoptotic cells. Therefore, annexin V detect the apoptotic cells with exposing phosphatidylserin to the outer cellular membrane. PI does not enter cells with intact cell membranes. In the results of flow cytometric analysis in present study, FaDu cell populations in both the late and early stages of apoptosis increased in a time-dependent manner to approximately 32.12% and 35.62% in response to 100 μM Lico-A treatment for 12 and 24 h, respectively. These findings indicate that Lico-A-induced FaDu cell death occurs through an apoptotic mechanism, a physiological process for killing cells. Therefore, apoptosis induced specifically in cancer cells is a promising target for chemotherapeutic drugs isolated from medicinal plants (Ko and Auyeung, 2013).

The extrinsic apoptotic pathway ligand TRAIL gradually initiated apoptosis in FaDu cells treated with Lico-A for 24 h, and subsequently activated its downstream pro-apoptotic factors caspase-8, caspase-7, caspase-3, and PARP. Furthermore, Lico-A-induced TRAIL expression in FaDu cells triggered the mitochondrial-dependent intrinsic apoptotic pathway, as indicated by the activation of pro-apoptotic factors such as tBid and caspase-9, expression of pro-apoptotic factors such as Bax, Bad, and Apaf-1, and the down-regulation of anti-apoptotic factors such as Bcl-2 and Bcl-xL. These events then induced FaDu cell apoptosis by activating caspase-3 and PARP as well as the extrinsic apoptotic pathway. Furthermore, Lico-A induced the activation of caspase-3 in a dose-dependent manner, whereas it was significantly counteracted by pan-caspase inhibitor Z-VAD-FMK. Moreover, caspase inhibitors such as Z-VAD-FMK (pan-caspase inhibitor), Z-IETD-FMK (caspase-8 inhibitor), or Z-LEHD-FMK (caspase-9 inhibitor) effectively rescued the Lico-A-induced apoptosis of FaDu cells. Although recently, Zeng et al., reported that mitochondria dependent intrinsic apoptosis signaling pathway involved with caspase-9 was dominant in SCC-25 oral cancer cells treated with Lico-A (Zeng et al., 2014). However, we did not observe the dominant apoptotic signaling pathways in either of them. These results suggested that Lico-A-induced apoptosis in FaDu cells are mediated by the activation of caspase-3 and occurs through both death receptor-mediated extrinsic and mitochondria-dependent intrinsic apoptotic pathways.

Recently, Kim et al. (2014) reported that Lico-A induced apoptosis in KB human oral cancer cells by stimulating a FasL-mediated extrinsic apoptotic pathway (Kim et al., 2014). Although we observed Lico-A-induced FasL expression in KB human oral cancer cells, we

did not observe FasL expression in FaDu cells stimulated with Lico-A (data not shown). We attribute this to cellular differences between FaDu and KB human oral cancer cells.

TRAIL, a ligand that initiates the process of apoptosis, was expressed in FaDu cells treated with Lico-A for 24 h in a dose-dependent manner. TRAIL binds to death receptors such as TRAIL-RI (death receptor 4) and TRAIL-RII (death receptor 5) located on the surfaces of cancer cells (de Jong et al., 2001). After TRAIL bound to these receptors, the death receptor adaptor protein FADD (Fas-Associated protein with death domain) induce the activation of caspase-8 and subsequently triggered both extrinsic and intrinsic apoptotic signaling pathways. To determine whether Lico-A-induced TRAIL expression was mediated by a MAPK signaling pathway, we showed that Lico-A induced the phosphorylation of ERK1/2 and p38 MAPK in FaDu cells. Yao et al. (2014) reported recently that Lico-A is a natural inhibitor of JNK MAPK and did not phosphorylate JNK in FaDu cells (Yao et al., 2014). Therefore, to verify which MAPK signaling pathway involved with Lico-A-induced expression of TRAIL, we examined TRAIL expression in FaDu cells treated with 100 μM Lico-A in both the presence and absence of 25 μM PD98059 (ERK1/2 inhibitor) and 5 μM SB203580 (p38 inhibitor). Lico-A significantly increased TRAIL expression in FaDu cells, whereas ERK1/2 and p38 chemical inhibitor suppressed significantly this effect of Lico-A. The levels of the downstream pro-apoptotic TRAIL targets caspase-8, -9, and -3, as well as PARP were significantly reduced by ERK1/2 and p38 inhibitors, suggesting that Lico-A-induced TRAIL expression was regulated by ERK1/2 and p38 MAPK signaling pathways. TRAIL regulated both extrinsic and intrinsic apoptotic pathways in FaDu cells, and Lico-A-induced FaDu cell death was completely inhibited by MAPK chemical inhibitors. Recently, Qu et al. (2011) reported that interferon-α sensitized human gastric cancer cells to TRAIL-induced apoptosis via activation of a c-CBL-dependent ERK MAPK pathway, and Lee et al. (2003) reported that interferon-γ-induced TRAIL expression was mediated by p38 MAPK in fetal brain astrocytes. Although we did not investigate the relationship between TRAIL expression and MAPK activation in the present study, these experiments are ongoing. Taken together, the expressional regulation of TRAIL might be a key regulator of apoptosis induction.

To perform an *in vivo* study, we generated a tumor animal model in which FaDu cells were xenografted. Tumors were significantly smaller in the xenografted group that had been administered Lico-A than those in the control group. Moreover, our immunohistochemical analysis of the tumors showed that caspase-3 activation was markedly increased in those injected with Lico-A. Although Yao et al. (2014) suggested that the anticarcinogenic effects of Lico-A in colon and pancreatic tumors was mediated by JNK MAPK inactivation, we showed that Lico-A-induced FaDu cell apoptosis was mediated by TRAIL-induced intrinsic and extrinsic apoptotic pathways.

5. Conclusion

In the present study, we demonstrated that Lico-A-induced cell death in FaDu cells depended on the activation of caspases involved in both intrinsic and extrinsic apoptotic pathways triggered by TRAIL expression. Furthermore, Lico-A induced the expression of TRAIL by activating both ERK1/2 and p38 MAPK signaling pathways (Fig. 6). Taken

together, these findings suggest that Lico-A, a potential therapeutic compound derived from natural herbal plants, can be used for the management of HNSCC.

Supplementary Material

Refer to Web version on PubMed Central for supplementary material.

Acknowledgements

Abbreviations

|	
Lico-A	Licochalcone-A
HNSCC	Head and neck squamous cell carcinoma
TRAIL	TNF-related apoptosis-inducing ligand
PARP	poly ADP-ribose polymerase
FasL	Fas ligand
FADD	Fas-associated protein with death domain
BID	BH3 interacting-domain death agonist
Bcl-2	B-cell lymphoma 2
Bcl-xL	B-cell lymphoma-extra large
Bax	Bcl-2-assiciated X protein
BAD	Bcl-2-assiciated death promoter
NHOK	Normal human oral keratinocytes
FBS	fetal bovine serum
MTT	3-(4, 5-dimethylthiazol-2-yl)-2, 5-diphenyl-tetrazolium bromide
DAPI	4'-6-diamidino-2-phenylinodole
PI	Propodium iodide
MAPK	mitogen activated protein kinase
DR	Death receptor

REFERENCES

Adianti M, Aoki C, Komoto M, Deng L, Shoji I, Wahyuni TS, Lusida MI, Soetjipto, Fuchino H, Kawahara N, Hotta H. Anti-hepatitis C virus compounds obtained from Glycyrrhiza uralensis and other Glycyrrhiza species. Microbiology and immunology. 2014; 58:180–187. [PubMed: 24397541]

Brake R, Starnes C, Lu J, Chen D, Yang S, Radinsky R, Borges L. Effects of palifermin on antitumor activity of chemotherapeutic and biological agents in human head and neck and colorectal carcinoma xenograft models. Molecular cancer research : MCR. 2008; 6:1337–1346. [PubMed: 18708365]
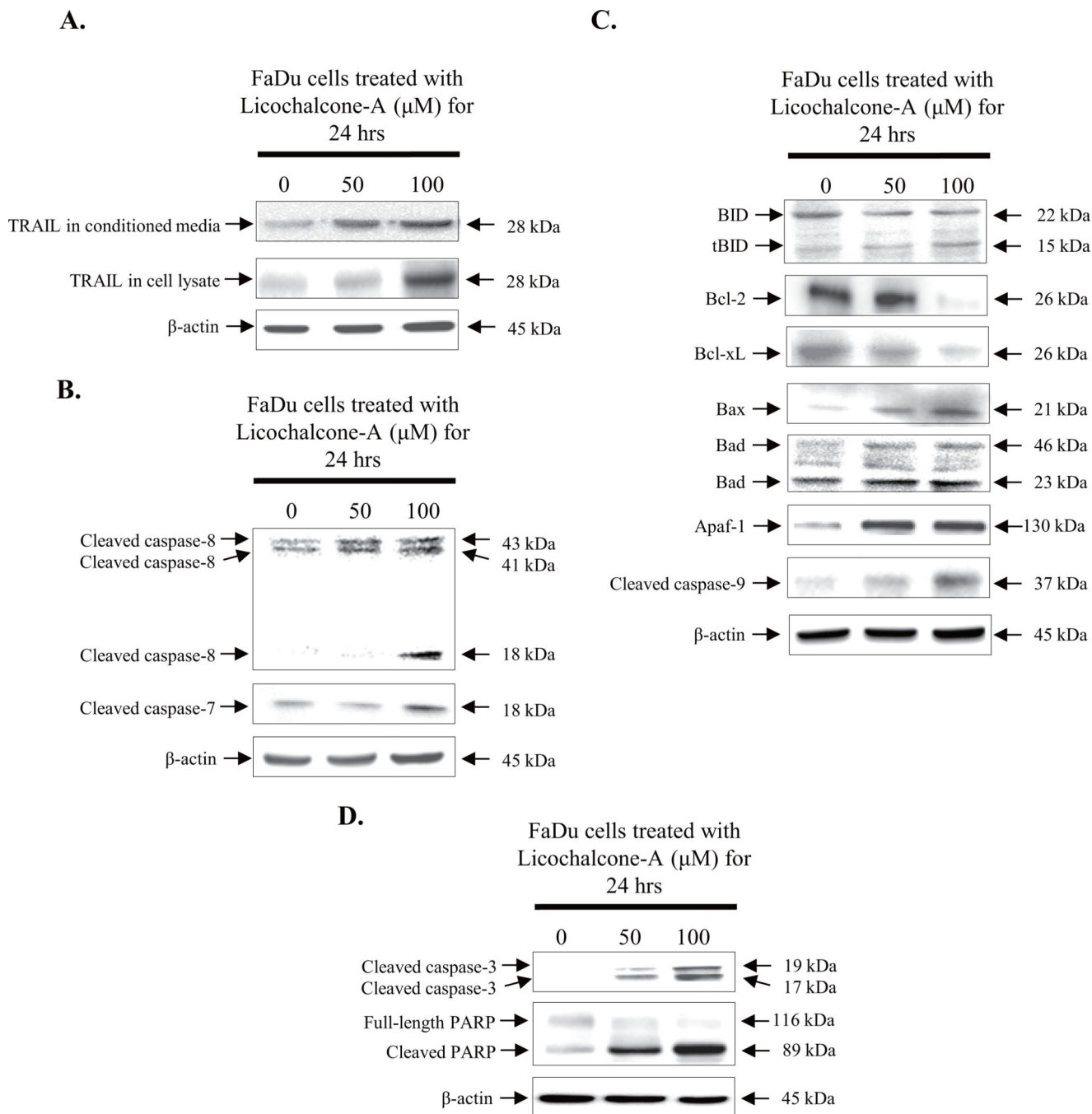
Chang EI, Leon P, Hoffman WY, Schmidt BL. Quality of life for patients requiring surgical resection and reconstruction for mandibular osteoradionecrosis: 10-year experience at the University of California San Francisco. Head & neck. 2012; 34:207–212. [PubMed: 21584893]

Cho JJ, Chae JI, Yoon G, Kim KH, Cho JH, Cho SS, Cho YS, Shim JH. Licochalcone A, a natural chalconoid isolated from Glycyrrhiza inflata root, induces apoptosis via Sp1 and Sp1 regulatory proteins in oral squamous cell carcinoma. International journal of oncology. 2014; 45:667–674. [PubMed: 24858379]

Choi AY, Choi JH, Hwang KY, Jeong YJ, Choe W, Yoon KS, Ha J, Kim SS, Youn JH, Yeo EJ, Kang I. Licochalcone A induces apoptosis through endoplasmic reticulum stress via a phospholipase Cgamma1-, Ca(2+)-, and reactive oxygen species-dependent pathway in HepG2 human hepatocellular carcinoma cells. Apoptosis : an international journal on programmed cell death. 2014; 19:682–697. [PubMed: 24337903]

Chu X, Ci X, Wei M, Yang X, Cao Q, Guan M, Li H, Deng Y, Feng H, Deng X. Licochalcone a inhibits lipopolysaccharide-induced inflammatory response in vitro and in vivo. Journal of agricultural and food chemistry. 2012; 60:3947–3954. [PubMed: 22400806]

de Jong S, Timmer T, Heijenbrok FJ, de Vries EG. Death receptor ligands, in particular TRAIL, to overcome drug resistance. Cancer metastasis reviews. 2001; 20:51–56. [PubMed: 11831647]

Dobrucki J, Darzynkiewicz Z. Chromatin condensation and sensitivity of DNA in situ to denaturation during cell cycle and apoptosis--a confocal microscopy study. Micron. 2001; 32:645–652. [PubMed: 11334733]

Fesik SW. Promoting apoptosis as a strategy for cancer drug discovery. Nature reviews. Cancer. 2005; 5:876–885. [PubMed: 16239906]

Fischer B, Coelho D, Dufour P, Bergerat JP, Denis JM, Gueulette J, Bischoff P. Caspase 8-mediated cleavage of the pro-apoptotic BCL-2 family member BID in p53-dependent apoptosis. Biochemical and biophysical research communications. 2003; 306:516–522. [PubMed: 12804595]

Fu Y, Chen J, Li YJ, Zheng YF, Li P. Antioxidant and anti-inflammatory activities of six flavonoids separated from licorice. Food chemistry. 2013; 141:1063–1071. [PubMed: 23790887]

Fu Y, Hsieh TC, Guo J, Kunicki J, Lee MY, Darzynkiewicz Z, Wu JM. Licochalcone-A, a novel flavonoid isolated from licorice root (Glycyrrhiza glabra), causes G2 and late-G1 arrests in androgen-independent PC-3 prostate cancer cells. Biochemical and biophysical research communications. 2004; 322:263–270. [PubMed: 15313200]

Hadden JW. The immunopharmacology of head and neck cancer: an update. International journal of immunopharmacology. 1997; 19:629–644. [PubMed: 9669203]

Hensley P, Mishra M, Kyprianou N. Targeting caspases in cancer therapeutics. Biological chemistry. 2013; 394:831–843. [PubMed: 23509217]

Hsan KM, Chen CC, Shyur LF. Current research and development of chemotherapeutic agents for melanoma. Cancers. 2010; 2:397–419. [PubMed: 24281076]

Huang AT, Georgolios A, Espino S, Kaplan B, Neifeld J, Reiter ER. Percutaneous endoscopic gastrostomy site metastasis from head and neck squamous cell carcinoma: case series and literature review. Journal of otolaryngology - head & neck surgery = Le Journal d'oto-rhino-laryngologie et de chirurgie cervico-faciale. 2013; 42:20.

Ikner A, Ashkenazi A. TWEAK induces apoptosis through a death-signaling complex comprising receptor-interacting protein 1 (RIP1), Fas-associated death domain (FADD), and caspase-8. The Journal of biological chemistry. 2011; 286:21546–21554. [PubMed: 21525013]

Jemal A, Bray F, Center MM, Ferlay J, Ward E, Forman D. Global cancer statistics. CA: a cancer journal for clinicians. 2011; 61:69–90. [PubMed: 21296855]

Kim JS, Park MR, Lee SY, Kim do K, Moon SM, Kim CS, Cho SS, Yoon G, Im HJ, You JS, Oh JS, Kim SG. Licochalcone A induces apoptosis in KB human oral cancer cells via a caspase-dependent FasL signaling pathway. Oncology reports. 2014; 31:755–762. [PubMed: 24337492]

Kim SN, Bae SJ, Kwak HB, Min YK, Jung SH, Kim CH, Kim SH. In vitro and in vivo osteogenic activity of licochalcone A. Amino acids. 2012; 42:1455–1465. [PubMed: 21468757]

Kim YH, Shin EK, Kim DH, Lee HH, Park JH, Kim JK. Antiangiogenic effect of licochalcone A. Biochemical pharmacology. 2010; 80:1152–1159. [PubMed: 20637733]

Kinghorn AD, Pan L, Fletcher JN, Chai H. The relevance of higher plants in lead compound discovery programs. Journal of natural products. 2011; 74:1539–1555. [PubMed: 21650152]

Ko JK, Auyeung KK. Target-oriented mechanisms of novel herbal therapeutics in the chemotherapy of gastrointestinal cancer and inflammation. Current pharmaceutical design. 2013; 19:48–66. [PubMed: 22950499]

Lacko M, Braakhuis BJ, Sturgis EM, Boedeker CC, Suarez C, Rinaldo A, Ferlito A, Takes RP. Genetic susceptibility to head and neck squamous cell carcinoma. International journal of radiation oncology, biology, physics. 2014; 89:38–48.

Lee CK, Son SH, Park KK, Park JH, Lim SS, Kim SH, Chung WY. Licochalcone A inhibits the growth of colon carcinoma and attenuates cisplatin-induced toxicity without a loss of chemotherapeutic efficacy in mice. Basic & clinical pharmacology & toxicology. 2008; 103:48–54. [PubMed: 18484961]

Lee CS, Kwak SW, Kim YJ, Lee SA, Park ES, Myung SC, Kim W, Lee MS, Lee JJ. Guanylate cyclase activator YC-1 potentiates apoptotic effect of licochalcone A on human epithelial ovarian carcinoma cells via activation of death receptor and mitochondrial pathways. European journal of pharmacology. 2012; 683:54–62. [PubMed: 22465181]

Li H, Zhu H, Xu CJ, Yuan J. Cleavage of BID by caspase 8 mediates the mitochondrial damage in the Fas pathway of apoptosis. Cell. 1998; 94:491–501. [PubMed: 9727492]

Li Y, Wang H, Wang Z, Makhija S, Buchsbaum D, LoBuglio A, Kimberly R, Zhou T. Inducible resistance of tumor cells to tumor necrosis factor-related apoptosis-inducing ligand receptor 2-mediated apoptosis by generation of a blockade at the death domain function. Cancer research. 2006; 66:8520–8528. [PubMed: 16951164]

Lin CC, Chuang YJ, Yu CC, Yang JS, Lu CC, Chiang JH, Lin JP, Tang NY, Huang AC, Chung JG. Apigenin induces apoptosis through mitochondrial dysfunction in U-2 OS human osteosarcoma cells and inhibits osteosarcoma xenograft tumor growth in vivo. Journal of agricultural and food chemistry. 2012; 60:11395–11402. [PubMed: 23066961]

Lin YS, Jen YM, Wang BB, Lee JC, Kang BH. Epidemiology of oral cavity cancer in taiwan with emphasis on the role of betel nut chewing. ORL; journal for oto-rhino-laryngology and its related specialties. 2005; 67:230–236.

Maier H, Dietz A, Gewelke U, Heller WD, Weidauer H. Tobacco and alcohol and the risk of head and neck cancer. The Clinical investigator. 1992; 70:320–327. [PubMed: 1521046]

McCarthy JV, Cotter TG. Cell shrinkage and apoptosis: a role for potassium and sodium ion efflux. Cell death and differentiation. 1997; 4:756–770. [PubMed: 16465288]

Messier C, Grenier D. Effect of licorice compounds licochalcone A, glabridin and glycyrrhizic acid on growth and virulence properties of Candida albicans. Mycoses. 2011; 54:e801–e806. [PubMed: 21615543]

Mishra LC, Bhattacharya A, Bhasin VK. Phytochemical licochalcone A enhances antimalarial activity of artemisinin in vitro. Acta tropica. 2009; 109:194–198. [PubMed: 19063856]

Osthus AA, Aarstad AK, Olofsson J, Aarstad HJ. Prediction of 5 year survival from level of perceived distress in newly diagnosed head and neck squamous cell carcinoma patients. Oral oncology. 2013; 49:964–969. [PubMed: 23830838]

Park SY, Kim EJ, Choi HJ, Seon MR, Lim SS, Kang YH, Choi MS, Lee KW, Yoon Park JH. Anti-carcinogenic effects of non-polar components containing licochalcone A in roasted licorice root. Nutrition research and practice. 2014; 8:257–266. [PubMed: 24944769]

Rothman KJ. Epidemiology of head and neck cancer. The Laryngoscope. 1978; 88:435–438. [PubMed: 628297]

Tao Q, Chan AT. Nasopharyngeal carcinoma: molecular pathogenesis and therapeutic developments. Expert reviews in molecular medicine. 2007; 9:1–24. [PubMed: 17477889]

Tounekti O, Belehradek J Jr, Mir LM. Relationships between DNA fragmentation, chromatin condensation, and changes in flow cytometry profiles detected during apoptosis. Experimental cell research. 1995; 217:506–516. [PubMed: 7535239]

Tsai JP, Hsiao PC, Yang SF, Hsieh SC, Bau DT, Ling CL, Pai CL, Hsieh YH. Licochalcone A suppresses migration and invasion of human hepatocellular carcinoma cells through

downregulation of MKK4/JNK via NF-kappaB mediated urokinase plasminogen activator expression. PloS one. 2014; 9:e86537. [PubMed: 24466137]

van Loo G, Schotte P, van Gurp M, Demol H, Hoorelbeke B, Gevaert K, Rodriguez I, Ruiz-Carrillo A, Vandekerckhove J, Declercq W, Beyaert R, Vandenabeele P. Endonuclease G: a mitochondrial protein released in apoptosis and involved in caspase-independent DNA degradation. Cell death and differentiation. 2001; 8:1136–1142. [PubMed: 11753562]

Vidal L, Gillison ML. Human papillomavirus in HNSCC: recognition of a distinct disease type. Hematology/oncology clinics of North America. 2008; 22:1125–1142. vii. [PubMed: 19010263]

Vigneswaran N, Wu J, Song A, Annapragada A, Zacharias W. Hypoxia-induced autophagic response is associated with aggressive phenotype and elevated incidence of metastasis in orthotopic immunocompetent murine models of head and neck squamous cell carcinomas (HNSCC). Experimental and molecular pathology. 2011; 90:215–225. [PubMed: 21236253]

Weissmann C. Fas ligand and Fas: a death factor and its receptor. Japanese journal of cancer research : Gann 85, inside front cover. 1994

Wittschier N, Faller G, Hensel A. Aqueous extracts and polysaccharides from liquorice roots (Glycyrrhiza glabra L.) inhibit adhesion of Helicobacter pylori to human gastric mucosa. Journal of ethnopharmacology. 2009; 125:218–223. [PubMed: 19607905]

Xiao XY, Hao M, Yang XY, Ba Q, Li M, Ni SJ, Wang LS, Du X. Licochalcone A inhibits growth of gastric cancer cells by arresting cell cycle progression and inducing apoptosis. Cancer letters. 2011; 302:69–75. [PubMed: 21216524]

Yao K, Chen H, Lee MH, Li H, Ma W, Peng C, Song NR, Lee KW, Bode AM, Dong Z, Dong Z. Licochalcone A, a natural inhibitor of c-Jun N-terminal kinase 1. Cancer prevention research. 2014; 7:139–149. [PubMed: 24253317]

Yo YT, Shieh GS, Hsu KF, Wu CL, Shiau AL. Licorice and licochalcone-A induce autophagy in LNCaP prostate cancer cells by suppression of Bcl-2 expression and the mTOR pathway. Journal of agricultural and food chemistry. 2009; 57:8266–8273. [PubMed: 19711916]

Yuan X, Li D, Zhao H, Jiang J, Wang P, Ma X, Sun X, Zheng Q. Licochalcone A-induced human bladder cancer T24 cells apoptosis triggered by mitochondria dysfunction and endoplasmic reticulum stress. BioMed research international. 2013; 2013:474272. [PubMed: 23936805]

Zeng G, Shen H, Yang Y, Cai X, Xun W. Licochalcone A as a potent antitumor agent suppresses growth of human oral cancer SCC-25 cells in vitro via caspase-3 dependent pathways. Tumour biology : the journal of the International Society for Oncodevelopmental Biology and Medicine. 2014; 35:6549–6555. [PubMed: 24691971]

Zhu J, Xiong L, Yu B, Wu J. Apoptosis induced by a new member of saponin family is mediated through caspase-8-dependent cleavage of Bcl-2. Molecular pharmacology. 2005; 68:1831–1838. [PubMed: 16183855]
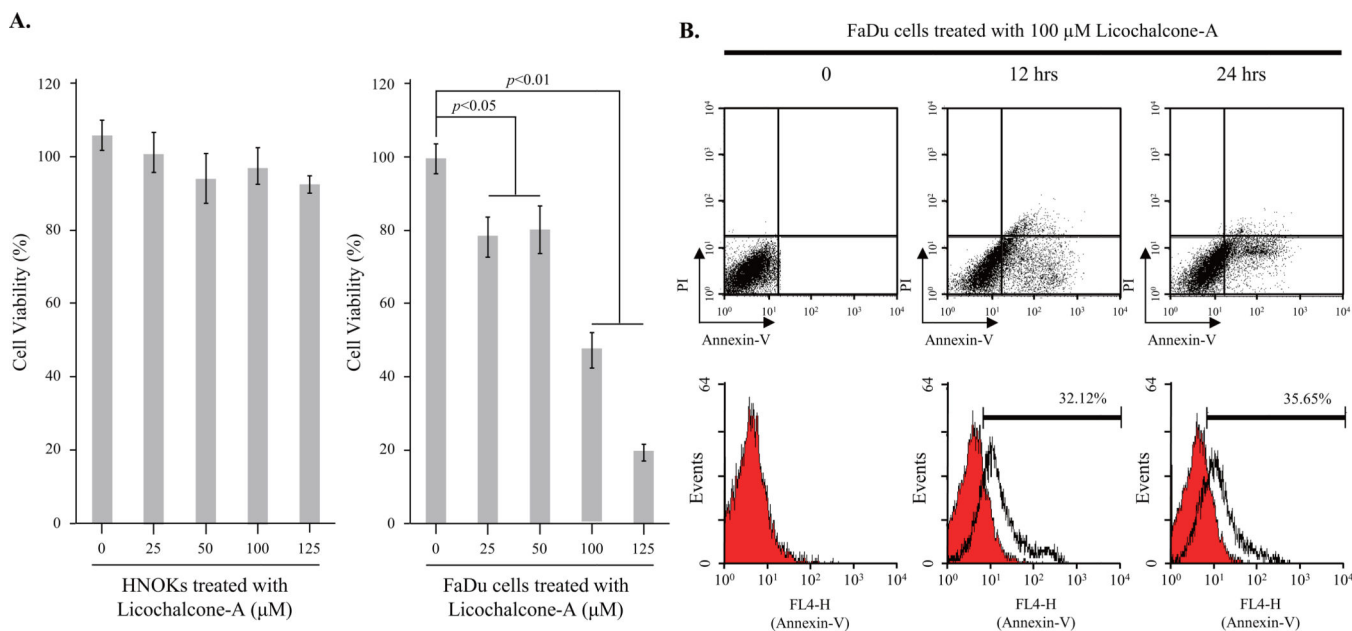
Fig. 1.
Licochalcone-A (Lico-A) selectively induces apoptotic cell death in FaDu cells, but not in human normal oral keratinocytes (hNOKs). (A) Lico-A has cytotoxic effects in FaDu cells, but not in hNOKs. hNOK and FaDu cells were treated with different doses of Lico-A (0, 25, 50, 100, and 125 μM) for 24 h. Under the indicated treatment conditions, cell viability was measured using an MTT assay. The data represent the results of three independent experiments and are expressed as the mean ± standard deviation (SD; *p < 0.05 and **p < 0.01 compared to the control). (B) Lico-A increases the apoptotic population in FaDu cells. To examine Lico-A-induced FaDu cell apoptosis, flow cytometric analysis was performed using annexin V and propidium iodide (PI) staining. FaDu cells were stimulated with 100 μM Lico-A for 12 and 24 h. After treatment, cells were analyzed by flow cytometry.

A.

FaDu cells treated with
Licochalcone-A (μM) for
24 hrs

	0	50	100	

TRAIL in conditioned media → ← 28 kDa

TRAIL in cell lysate → ← 28 kDa

β-actin → ← 45 kDa

B.

FaDu cells treated with
Licochalcone-A (μM) for
24 hrs

	0	50	100	

Cleaved caspase-8 → ← 43 kDa
Cleaved caspase-8 → ← 41 kDa

Cleaved caspase-8 → ← 18 kDa

Cleaved caspase-7 → ← 18 kDa

β-actin → ← 45 kDa

C.

FaDu cells treated with
Licochalcone-A (μM) for
24 hrs

	0	50	100	

BID → ← 22 kDa
tBID → ← 15 kDa

Bcl-2 → ← 26 kDa

Bcl-xL → ← 26 kDa

Bax → ← 21 kDa

Bad → ← 46 kDa

Bad → ← 23 kDa

Apaf-1 → ← 130 kDa

Cleaved caspase-9 → ← 37 kDa

β-actin → ← 45 kDa

D.

FaDu cells treated with
Licochalcone-A (μM) for
24 hrs

	0	50	100	

Cleaved caspase-3 → ← 19 kDa
Cleaved caspase-3 → ← 17 kDa

Full-length PARP → ← 116 kDa

Cleaved PARP → ← 89 kDa

β-actin → ← 45 kDa

Fig. 2.
Lico-A-induced FaDu cell death is mediated by both intrinsic and extrinsic apoptotic pathways. FaDu cells were treated with 50 and 100 μM Lico-A for 24 h. After treatment, both total protein and conditioned media were harvested FaDu cells and then western blots were performed. (A) Lico-A increases TRAIL expression in both cell lysate and conditioned media as a dose-dependent manner. (B) Lico-A induces the extrinsic apoptotic signaling pathway. (C) Lico-A induces the intrinsic apoptotic signaling pathway. (D) Lico-A induces FaDu cell death by activating caspase-3 and poly (ADP ribose) polymerase (PARP).
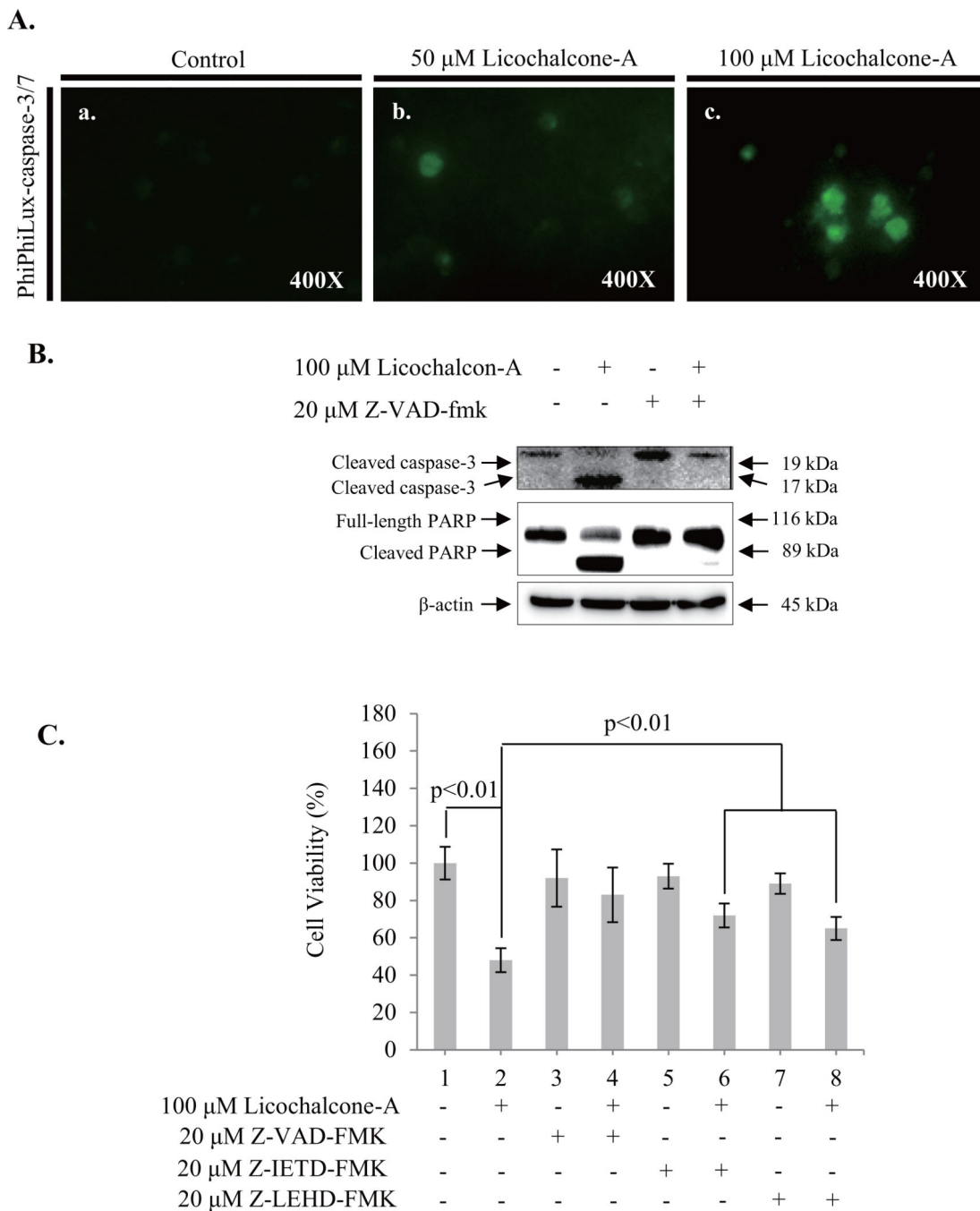
A.

B.

C.

Fig. 3.
Lico-A-induced apoptosis in FaDu cells is dependent on caspase activation. (A) Lico-A induces the caspase-3/-7 activation in FaDu cells. A caspase-3/-7 intracellular activity assay was performed using PhiPhiLux-caspase-3/-7 substrate. The stained FaDu cells were observed and imaged using an inverted phase-contrast microscope. (B) Z-VAD-FMK, a pan-caspase inhibitor, inhibited Lico-A-induced activation of caspase-3/-7 and PARP in FaDu cells. FaDu cells were stimulated with Lico-A in presence or absence in Z-VAD-FMK for 24 h. After treatment, total protein was extracted and western blotting was performed to

assess the activation of caspase-3/-7 and PARP. (C) The inhibition of caspase activation suppresses Lico-A-induced cytotoxicity in FaDu cells. FaDu cells were stimulated with Lico-A in the presence or absence in Z-VAD-FMK (pan-caspase inhibitor), Z-IETD-FMK (caspase-8 inhibitor), or Z-LEHD-FMK (caspase-9 inhibitor) for 24 h. Cell cytotoxicity was measured by MTT assay.

A.

B.

C.
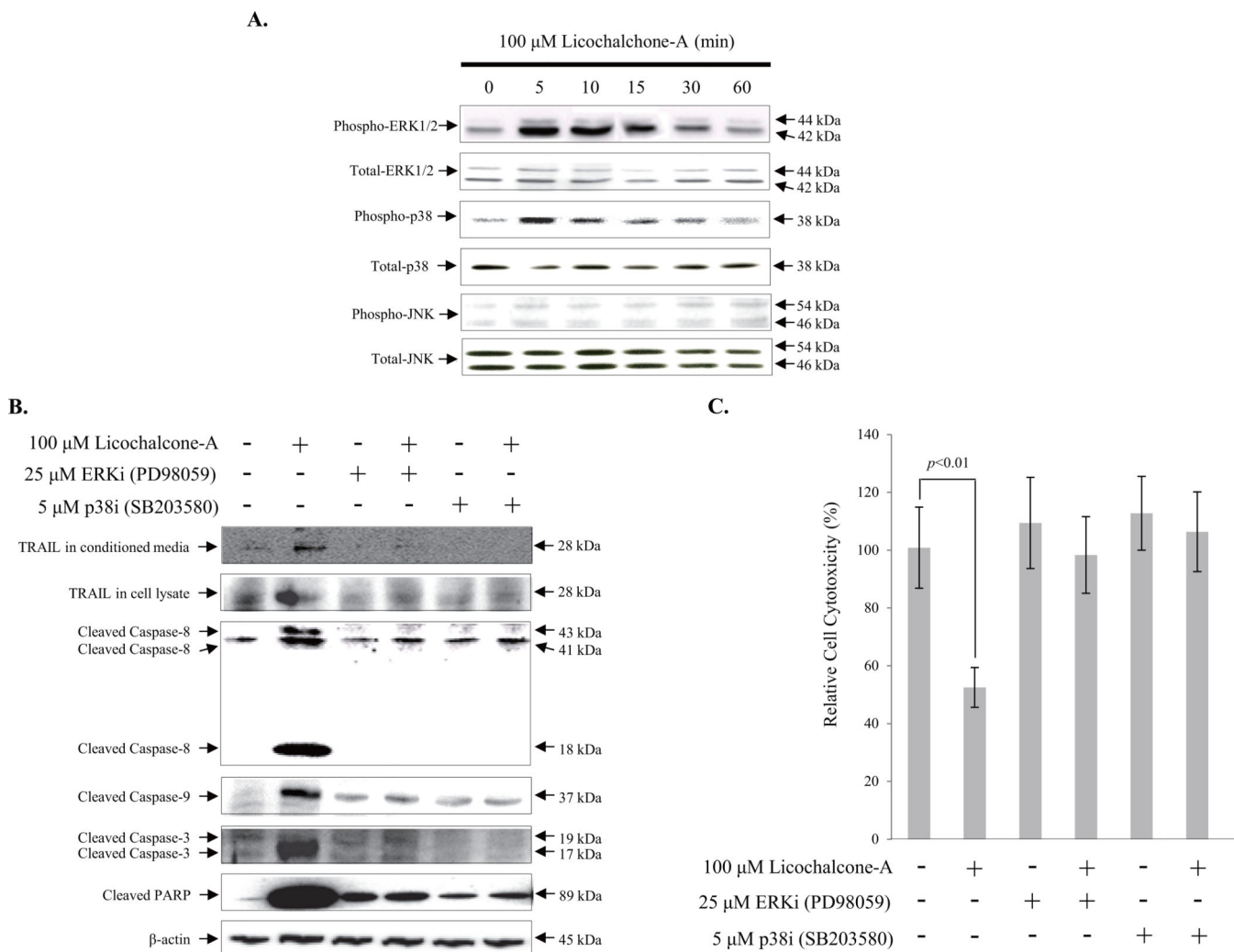
Fig. 4.
Lico-A-induced FaDu cell apoptosis is regulated by TRAIL expression induced by ERK1/2 and p38 MAPK phosphorylation. (A) Lico-A induced the phosphorylation of both ERK1/2 and p38 MAPK, but not JNK MAPK in FaDu cells. FaDu cells were stimulated with 100 μM Lico-A for the indicated treatment times. After treatment, total protein was extracted and western blotting was performed to detect the MAPK activation. (B) Lico-A induces TRAIL expression via ERK1/2 and p38 MAPK signaling pathways in FaDu cells. FaDu cells were treated with 100 μM Lico-A in the presence or absence of 25 μM PD98059 (ERK1/2 inhibitor) and 5 μM SB203580 (p38 inhibitor) for 24 h. After treatment, total protein was extracted and western blotting was performed to assess the changes in TRAIL, caspase-8, caspase-9, caspase-3, and PARP expression. (C) Inhibition of the ERK1/2 and p38 MAPK signaling pathways suppresses the Lico-A-induced FaDu cell apoptosis. FaDu cells were treated with 100 μM Lico-A in the presence or absence of 25 μM PD98059 and 5 μM SB203580 for 24 h. After treatment, cell cytotoxicity was measured by MTT assay.

A.

B.

C.
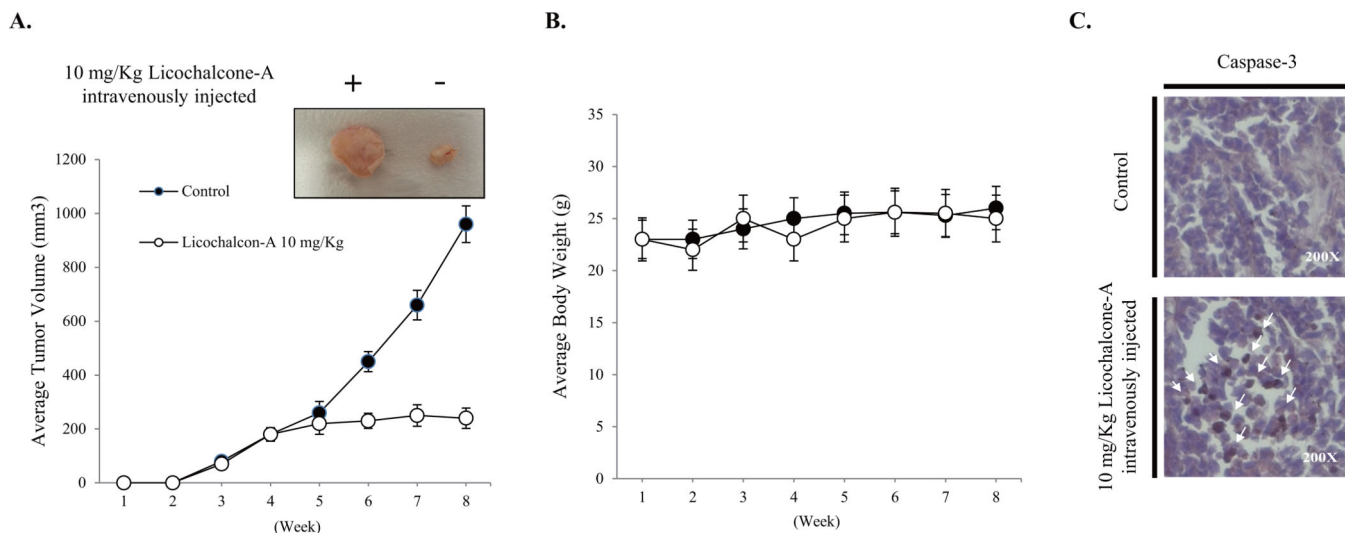
Fig. 5.

Lico-A inhibits the volume of FaDu tumors in a xenografted animal model. (A) Lico-A significantly reduces tumor volume in a FaDu xenograft animal model. Lico-A (10 mg/kg) and vehicle were intravenously injected into experimental and control groups, respectively, three times per week for 8 consecutive weeks. Tumor sizes were measured using a caliper prior to intravenous injections. (B) Lico-A (10 mg/kg) has no effect on animal body weight. (C) Lico-A (10 mg/kg) induces the activation of caspase-3 in tumor tissue collected from FaDu cell xenografted animals. After the treatment period, tumor tissues were dissected from xenografted animals perfused and fixed using saline and 4% paraformaldehyde, respectively. Dissected tumor tissues were post-fixed using 4% paraformaldehyde and were embedded in paraffin for sectioning. Immunohistochemistry was performed using caspase-3 antibody as described in the Materials & Methods. Sections were counterstained using hematoxylin and eosin. Immunoreactive cells are indicated by white arrows.
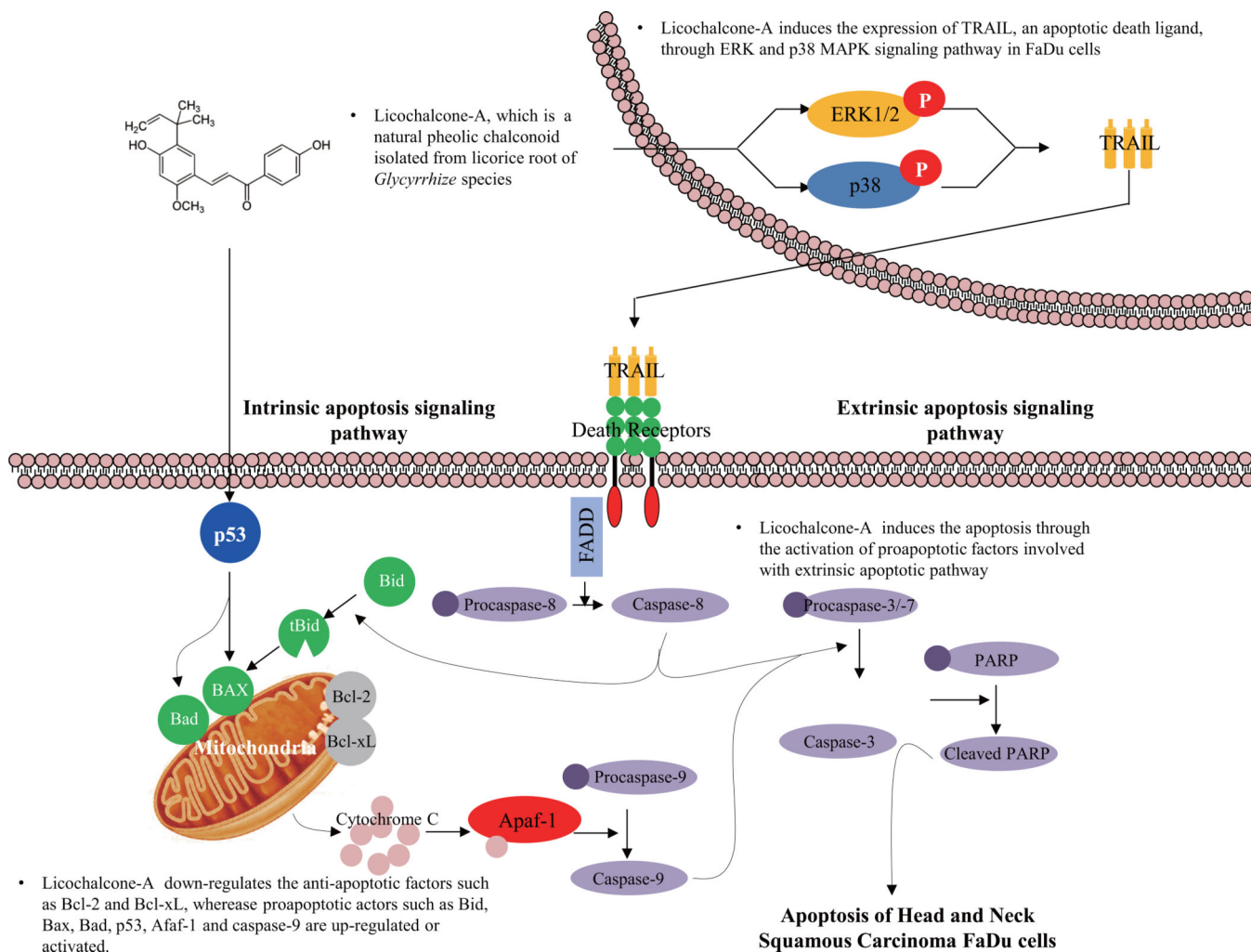
Fig. 6.
Apoptotic signaling pathway induced by Licochalcone-A in head and neck squamous carcinoma FaDu cells.